Proceedings World Geothermal Congress 2015
Melbourne, Australia, 19-25 April 2015

Thermo-Hydro-Mechanical-Chemical Coupled Modeling of Geothermal Doublet Systems in Limestones

Wolfram Rühaak[1], Liang Pei[1], Jörn Bartels[2], Claus-Dieter Heldmann[1], Sebastian Homuth[3], Ingo Sass[1]

[1]Technische Universität Darmstadt, Geothermal Science and Technology, Schnittspahnstrasse 9, D-64287 Darmstadt/Germany

[2]Geothermie Neubrandenburg GmbH, Seestraße 7a, D-17033 Neubrandenburg/Germany

[3]Züblin Spezialtiefbau GmbH, Europa-Allee 50, D-60327 Frankfurt a.M./Germany

ruehaak@geo.tu-darmstadt.de

Keywords: THMC, limestone, injectivity, thermal expansion coefficient, numerical modeling

ABSTRACT

Limestone aquifers in Southern Germany have been used within the last decade very successfully for geothermal heating and – to a lesser extent – for power generation. As an example the region around Munich has been extensively explored. While the extent of usage of this reservoir is increasing there is also an increased interest in better understanding of the reservoir properties and its change in the course of operation. For instance, the observed production and injection pressures are partly hard to explain. They may be related to mechanical or chemical processes, or both.

Based on extensive data of outcrop studies and drillings, a data-base for the relevant physical properties of the respective limestones has been complied. The data include thermal conductivity, density, specific heat capacity, permeability, as well as mechanical properties like thermal expansion coefficient and elasticity modules.

By using the hydro-thermo-chemical simulator FEFLOW together with an extension for thermo- and hydro-mechanical coupling the relevant processes are studied and compared with observed data. Conclusions for an optimized operation of geothermal systems in limestones are given and discussed.

1. INTRODUCTION

A geothermal doublet is the simplest type of a deep and open system for getting hot water from the subsurface. Earths' heat is subsequently taken from the fluid pumped from one borehole to the power plant cycle and considerably cooled water is then reinjected in another borehole.

The injection is typically performed in the same geological unit like the extraction. The reason for using such an additional and accordingly costly deep well is mainly to maintain the original water pressure in the reservoir. Furthermore it is possible to interchange extraction and injection wells; another important reason is that the chemistry of the injected fluid is in equilibrium with the groundwater. In cases of disequilibrium reservoir scaling is likely to occur, and the resulting decrease of injectivity could jeopardize a project. Building an extraction-reinjection system is the prerequisite to avoid land depressions due to leaching and for a sustainable reservoir operation.

Limestone aquifers in southern Germany have been used within the last decade very successfully for geothermal heating and – to a lesser extent – for power generation. For instance the region around Munich has been extensively explored. While the usage of this reservoir is increasing there is also an increased interest in better understanding the reservoir properties. For instance observed pumping rates and injection pressures are partly hard to explain. They may be related to mechanical or chemical processes, or both.

Based on extensive data of outcrop studies and drillings a data-base for the relevant physical properties of the respective limestones have been complied. This includes thermal conductivities, density, specific heat capacity, permeability as also mechanical properties like thermal expansion coefficient and elasticity modules.

The study focuses on available techniques and current limitations in 2D/3D modelling of a fracture in a limestone. Based on a presumed fracture aperture the flow inside can be modelled, for instance by using the cubic law approach (Snow, 1965). Into this fracture relatively cold water is injected. Differences in temperature are an important source of stresses and deformations in solid bodies; only direct strains and no shear strains are produced by the temperature differences (Pepper and Heinrich, 2005). Thermal expansion of a fracture causes a spatially and temporally varying aperture. Additionally, direct and shear strain occur due to the increased pressure resulting from pumping. Both processes increase the aperture width.

In addition chemical dissolution as a function of pressure and temperature of the aquifer may occur; as said, the chemistry is presumed to be in equilibrium.

For studying the possible effects due to the injection of cold water into the limestone reservoir rocks, similar rocks from analogue outcrops where collected and respective values for the thermal expansion where measured in the laboratory.

2. OBSERVED INJECTIVITY AND PRODUCTIVITY DATA

For a few hydrogeothermal wells tapping the Upper Jurassic reservoir of the Bavarian Molasse Basin both measured injectivity and productivity data are available. A comparison of these data could provide a hint that pressure dependence of hydraulic conductivity in the vicinity of the wells is a significant feature in the parameter range where these geothermal wells are operated.

Generally, this aquifer is of fractured/karstified – porous type. But the main inflow sections of the wells are usually in connection with fractured fault zones.

Well productivity (productivity index PI = production rate/bottom hole drawdown) and injectivity (injectivity index II = injection rate/bottom hole pressure increase) are influenced by a series of processes as listed in Table 1.

Table 1 Overview of near well reservoir processes effecting productivity and injectivity of a geothermal well in a fractured-porous carbonate reservoir.

	Process	Possible effect on productivity	Possible effect on injectivity
1	Carbonate transport by near well dissolution in cold water and far well precipitation		Long term II increase
2	Variation of fracture aperture at well inflow by pressure variation	Short term PI reduction	Short term II improvement
3	Increase of fracture aperture by rock cooling		Short term II improvement
4	Decrease of hydraulic conductivity around the injection well by increase of reservoir fluid viscosity caused by cooling		Short term II reduction
5	Transition from laminar to turbulent flow regime near the well at high flow rates	Short term PI reduction	Short term II reduction

To separate the effect of near well pressure on productivity and injectivity (process 2) the effects of the other four processes have to be excluded. Process 1 acts long term, i.e. short term tests up to some weeks should not be influenced. Far well precipitation is expected but due to the distance it is unlikely that it leads to a decrease of injectivity. To eliminate the effect of temperature (process 3 and 4) only injection tests without cooling should be used (doublet circulation test). One exception has been made with a data set from two very short term single well production and injection and test where cold water was injected. Due to the warming of the injected water along the well path of depth larger than 3000 m measured injection temperature was 120 °C – 80 °C. To eliminate the effect of process 5 injectivity and productivity have to be measured at similar flow rates.

Figure 1 shows the II-PI-ratio of the 2 times 5 hydraulic test results found. They all fulfil the criteria above. All measurements are from downhole pressure gauges. This excludes influences from temperature dependent density of the water column and friction losses in the well.

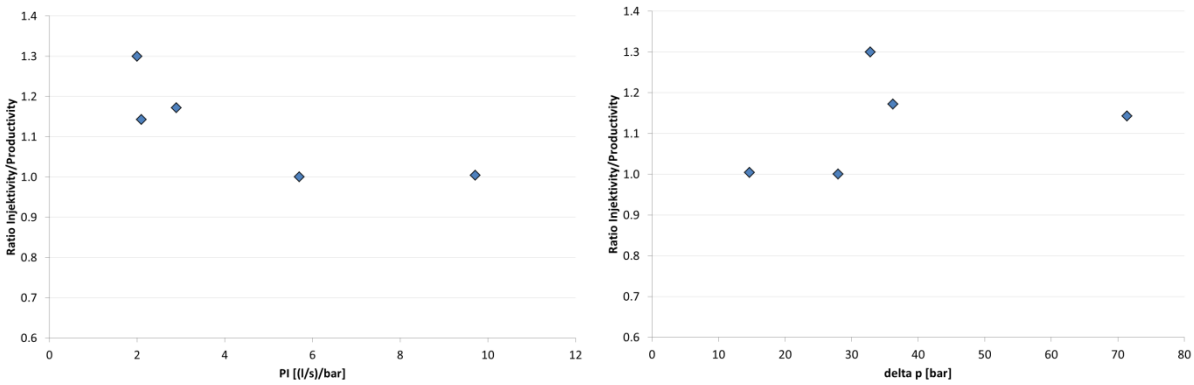

Figure 1 Observed ratio of injectivity and productivity of five geothermal wells developing the Upper Jurassic aquifer of the Bavarian Molasse Basin plotted vs. PI (left) and vs. difference of downhole well pressure (delta p) at production and injection (right).

The main result is that no ratio smaller than 1 is observed, i.e. injectivity has been larger than productivity in all available test data sets. This could be a hint that pressure could influence hydraulic conductivity in the vicinity of these geothermal wells. It seems that injectivity is only higher than productivity at low to medium PI values. The two very productive wells (PI > 5) do not show this effect. This could be caused by the smaller initial (delta p = 0) fracture aperture at wells with low productivity. Furthermore, the total difference between downhole well pressure at injection and production is smallest for the two wells with II/PI=1. The highest II/PI-ratio (1.3) is obtained from the data set of the above mentioned short term tests. In accordance with the argumentation above this should be caused by the fact that this well also has the lowest absolute productivity. But it is also possible that it is an additional hydraulic conductivity improvement by rock cooling (process 3 in Table 1).

3. GEOLOGY

The shallow-water areas of inner carbonate ramps are generally well known from a larger number of case studies (Wright and Burchette, 1998), partly because of the availability of actualistic analogs (Kirkham, 1998, Pawellek and Aigner, 2003) studied

especially for the hydrocarbon exploration. In contrast, the deeper-water zones of outer carbonate ramp systems received comparatively little attention and are now in the focus of the geothermal exploration in the Molasse Basin in Southern Germany.

During the Mesozoic, large parts of the European craton were covered with a shelf sea marginal to the Tethys Ocean in the South. In the North, this shelf sea was separated from the boreal sea by an island archipelago of changing dimensions. An extensive siliceous sponge–microbial reef belt has been developed. With the burial of the Vindelician Ridge a direct connection of the south German Jurassic Sea with the Tethys Ocean was established (Meyer and Schmidt-Kaler, 1989). During the entire Upper Jurassic a high carbonate production on the shallow shelf resulted in thick limestone series (Selg and Wagenplast, 1990). In the southern, deeper part of this epicontinental shelf sea, a reefal facies, established in the Middle Oxfordian, was part of an intensive facies belt characterized by frequent silicious sponge reefs spanning the northern Tethys shelf (Pieńkowski et al., 2008). In addition, clay-rich sediments from the Mid German Swell were shed into the shelf area. During times of low carbonate production, the clay content of the sediments increased which resulted in the sedimentation of marl (Meyer and Schmidt-Kaler, 1990). These differences in facies are reflected in the different development of the carbonate successions of the Swabian and Franconian Alb and their southern adjacent buried sections in the Molasse Basin. According to Meyer and Schmidt-Kaler (1989, 1990), the Swabian facies as the central part of the reef belt formed a deeper-water area between the shallower Franconian–Southern Bavarian platform in the East and the Swiss platform in the West. To the South, the Swabian facies passed into the Helvetic Basin. The Helvetic facies is characterized by dense typically dark and bituminous limestones with in places interbedded oolith layers. This facies describes the transition of the Germanic facies into the Helvetic facies, which is considered as sediments of a deeper shelf area of bedded limestones with very low permeabilties. Also karstification is not observed, so the northern boundary of the Helvetic facies is considered as the southern boundary of the Upper Jurassic aquifer of the Molasse Basin (Villinger, 1988).

In general 400 m to 600 m of carbonate rocks were deposited during the Upper Jurassic. Two major lithofacies-types can be distinguished (Geyer and Gwinner, 1979, Pawellek and Aigner, 2003):

(1) a basin facies, consisting of wellbedded limestones and calcareous marls (mud-/wackestones), and
(2) a reefal or massive facies, when bedding is either absent, indistinct or very irregular (rud-/float-/grainstones).

The massive limestones are built by microbial crusts (stromatolites and thrombolites) and siliceous sponges that have been interpreted by various authors as relatively deep and quiet water ‘reefs’, mounds or bioherms (Gwinner, 1976, Leinfelder et al., 1994, 1996, Pawellek and Aigner, 2003). The normal facies may either interfinger with the reefs or onlap onto the reefs (Gwinner, 1976, Pawellek, 2001). In the upper parts of the Upper Jurassic, a coral facies developed locally upon the microbial crust–sponge reefs. The abundance of reef facies differs regularly through time. Reef expansion phases correlate with an increase in the carbonate content within the basin facies, while phases of reef retreat correlate with increasing abundance of marls within the basin facies (Meyer and Schmidt-Kaler, 1989,1990, Pawellek, 2001).

To cover the variety of different reservoir rock types over several stratigraphic units, major facies types and according lithotypes a set of samples from suitable outcrop locations spanning from Malm alpha to zeta were tested in terms of their thermophysical (250 samples) and geomechanical (50 samples) properties (Homuth et al., 2014).

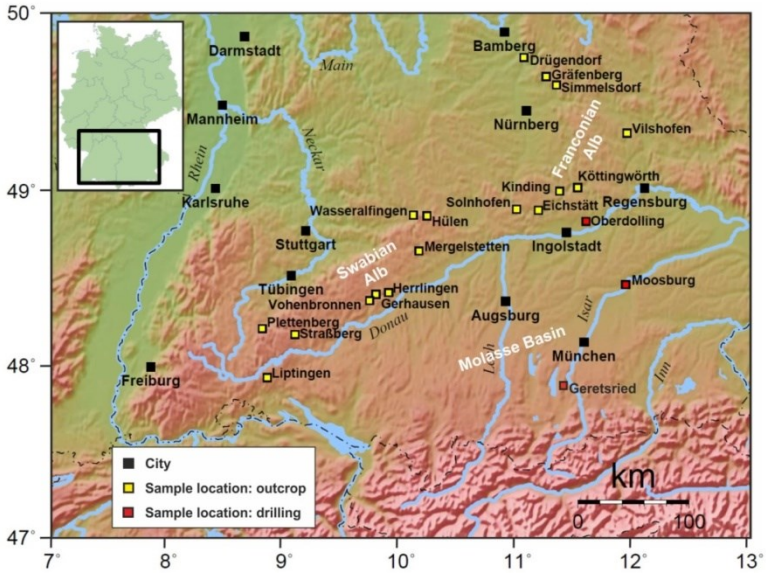

Figure 2: Study area with location of studied outcrops of the analogues Swabian and Franconian Alb and drillings within the Molasse Basin (Homuth et al. 2014).

4. MEASUREMENT OF THERMAL EXPANSION COEFFICIENT OF LIMESTONE

Using the thermo-triaxial device in Darmstadt (Pei et al., 2014), the expansion coefficients of 6 rock specimens of different lithotypes were measured under given stress conditions. The test procedures were as follows: (a) Initial vertical stress of 15 MPa and confining pressure of 10 MPa were applied on the rock specimen; (b) The rock specimen was heated up to 150 °C at a heating rate of 10 °C per hour. The temperature was subsequently kept constant till the readings of the lateral extensometer became stable.

Afterwards the temperature was ramped down to 20 °C and kept constant till the rock specimen did not contract further (Fig. 3); (c) The circumference change of rock specimen during heating and cooling was detected and recorded by a lateral extensometer and then it was converted into diameter change and the change of lateral strain.

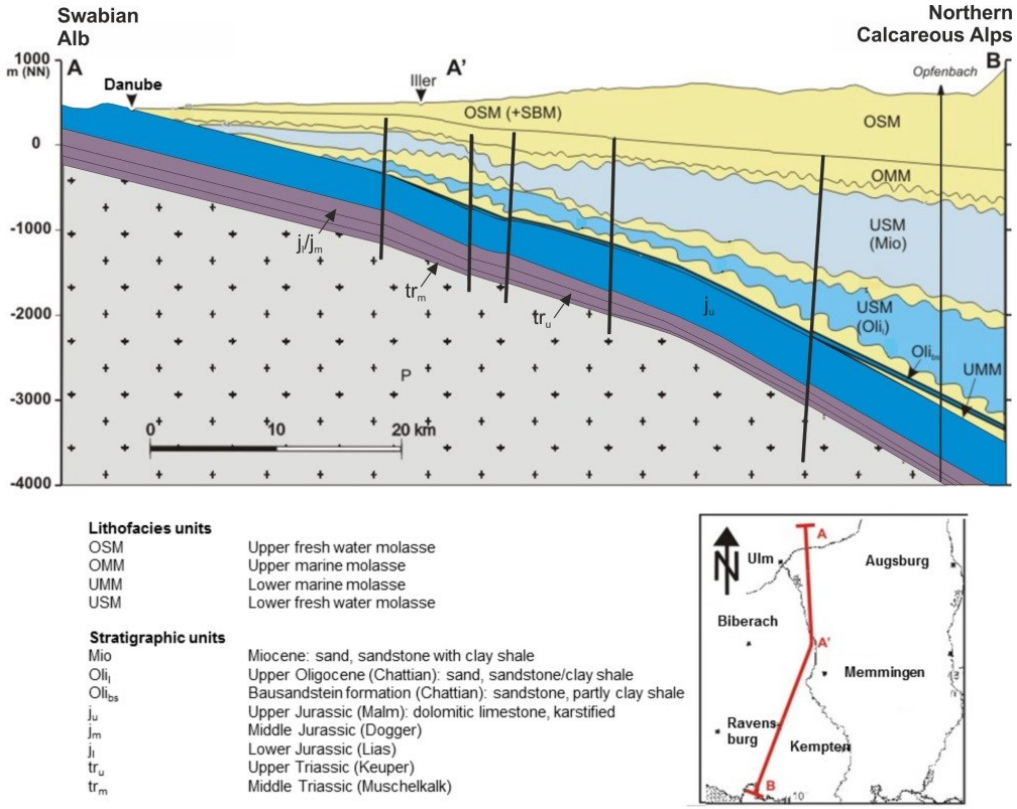

Figure 3 Cross section of the western Molasse Basin (modified, Clauser et al. 2002)

In Fig. 3 it is observed that the rock specimen neither only expands during heating nor only contracts during cooling. The phenomenon can be ascribed to the fact that the chain-shaped lateral extensometer is sensitive to temperature and contributes to the readings of the circumference change. By analyzing the derivative of the circumference change curve, the influence from the expansivity of the lateral extensometer was eliminated. The calibrated values of lateral strain are plotted in Fig. 4 and the gradients of the linear curves indicate the thermal expansion coefficients of each rock specimen during heating and cooling (Tab. 1). The diameter of rock specimen at the end of initial loading (σ_1 = 15 MPa, σ_3 = 15 MPa, 20 °C) was taken as the original diameter, on which the calculation of lateral strain is based. According to Fig. 4, the lateral strain of rock specimen does not recover at the end of cooling, resulting in lower values of thermal expansion coefficient for cooling stage (Tab. 1). A possible reason could be that the anisotropy of thermal expansion of calcite, which is the dominant mineral component of limestone, together with the existing vertical stress and confining pressure have induced plastic change in the rock specimen during temperature cycles. Hence the plastic change accounts for part of the lateral strain developed in the heating stage, while the less obvious lateral strain developed in cooling stage and the corresponding thermal expansion coefficients manifest the intrinsic expansivity of the rock matrix. However the reliability of the explanation should be verified with further experiments and analyses.

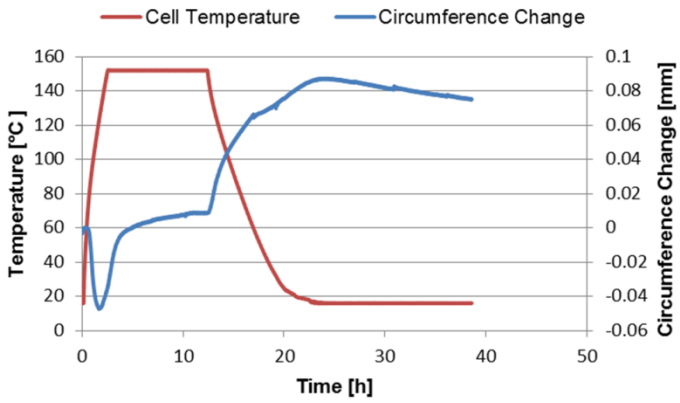

Figure 4: Thermal-triax test procedure of measurement of thermal expansion coefficient of limestone.

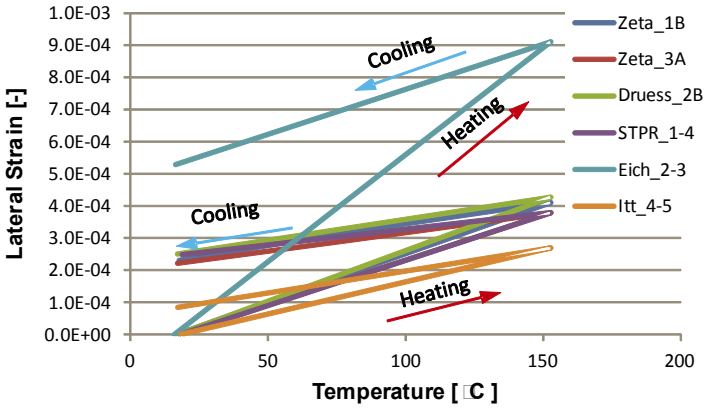

Figure 5: Lateral strain of limestone during heating and cooling.

Table 2: Thermal Expansion Coefficient of Limestone.

Sample	α_Heating [°C^{-1}]	α_Cooling [°C^{-1}]
Zeta_3A	2.8E-06	1.2E-06
Zeta_1B	3.0E-06	1.3E-06
Druess_2B	3.1E-06	1.3E-06
STPR_1-4	2.8E-06	9.8E-07
Itt_4-5	2.0E-06	1.4E-06
Eich_2-3	6.7E-06	2.8E-06

5. THERMO-HYDRO-MECHANICAL-CHEMICAL MODELING

The general concept of thermo-hydro-mechanical-chemical coupling is depicted in Figure 6. A description of hydro-mechanical coupling requires simultaneous solution of equations for groundwater flow (Darcy equation) and the mechanical behavior described, for instance following Biot (1941). For thermo-coupling, the heat-transport equation also has to be coupled dynamically. Chemical coupling requires the inclusion of mass-transport, sorption, solution and precipitation.

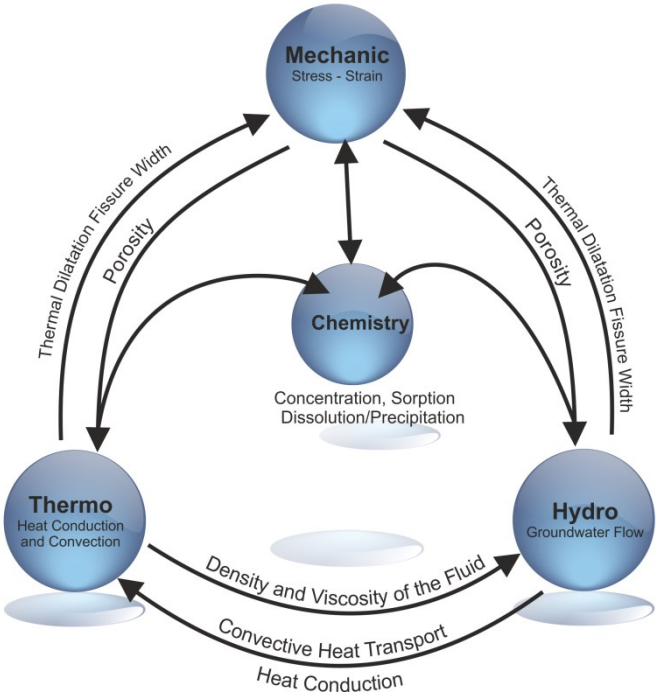

Figure 6: Thermo-hydro-mechanical coupling and the respective constitutive laws.

In recent years the inclusion of thermal effects into the theory of hydro-mechanical (HM) coupling has become increasingly prevalent (e.g. Lee and Ghassemi, 2011, Rühaak and Sass, 2013). Important applications are for instance the modelling of thermo-mechanical (TM) processes in nuclear waste disposal assessments. In addition, thermo-hydro-mechanical (THM) induced stress-strain can have an impact on processes related to the performance of geothermal reservoirs. For computing such processes numerically on the respective relevant scales, stress-strain relationships resulting from fluid pressure and temperature have to be computed and dynamically coupled to the regional flow and transport regime.

A prototypical application of THM codes is for instance the productivity of a geothermal doublet system with one pumping well and one injection well, which can be influenced by mechanical changes and associated change in hydraulic conductivity (Bundschuh and Suárez-Arriaga, 2010). General reviews of THM coupled processes are given in Wang et al. (2009), Watanabe et al. (2010) and Kolditz et al. (2012).

Thermo-mechanical coupling is generally unidirectional as thermal expansion induces volume changes of the rock (similar to pore pressure changes in case of hydro-mechanical coupling); vice versa the mechanics do not alter the temperature directly but only due to changes of the (convective) flow field.

5.1 THMC Continuity equations

For THMC coupled modelling, the following continuity equations have to be solved (Bear, 1972, Kinzelbach, 1992, Diersch and Perrochet, 1999, Alberty et al., 2002, Ingebritsen et al., 2006, Rühaak et al., 2008, Rühaak et al., 2014):

Groundwater flow

$$S_S \frac{\partial h}{\partial t} = \nabla \cdot (\mathbf{K} \nabla h) + \alpha_b \frac{\partial \varepsilon_{vol}}{\partial t} \tag{1}$$

where S_S is the storage coefficient (m^{-1}), h is hydraulic head (m), t is time (s), α_b (-) is the Biot coefficient, an empirical constant (Biot, 1941) ranging from 0 to 1, describing to which extent fluid pressure counteracts elastic deformation of porous rock (Alam et al., 2010), $\partial \varepsilon_{vol} / \partial t$ is the time rate of change of volumetric strain (s^{-1}) and $\mathbf{K}$ is the hydraulic conductivity tensor ($m\ s^{-1}$), according to

$$\mathbf{K} = \frac{\mathbf{k} \rho g}{\eta} \tag{2}$$

where $\mathbf{k}$ is the permeability tensor (m^2), ρ is density ($kg\ m^{-3}$), g is gravity ($m\ s^{-2}$) and η is the dynamic viscosity ($kg \cdot m^{-1} \cdot s^{-1}$).

The resulting groundwater flow expressed by the Darcy velocity $\mathbf{q}$ ($m\ s^{-1}$) is

$$\mathbf{q} = -\mathbf{K} \cdot \nabla h \tag{3}$$

Coupled conductive and convective heat-transport is expressed by

$$(\rho c)_s \frac{\partial T}{\partial t} = \nabla \cdot (\boldsymbol{\lambda}_T \nabla T - (\rho c)_f \mathbf{q} T) \tag{4}$$

where $(\rho c)_s$ is the bulk volumetric heat ($J\ K^{-1}\ m^{-3}$), T is temperature (°C), $\boldsymbol{\lambda}_T$ is the thermal conductivity tensor ($W\ m^{-1}\ K^{-1}$), index f denotes fluid properties.

Linear elasticity equation is given by

$$(\lambda + \mu) \nabla \nabla \cdot \mathbf{u} + \mu \nabla^2 \mathbf{u} = -\mathbf{f} \tag{5}$$

where $\mathbf{u}$ is the displacement vector (m), and $\mathbf{f}$ is the volume force (N), typically resulting from the pore pressure, and λ is Lamé's first parameter (MPa).

Eq. 5 is combined with the stress-strain relationship

$$\begin{bmatrix} \sigma_x \\ \sigma_y \\ \sigma_z \\ \tau_{xz} \\ \tau_{yx} \\ \tau_{zy} \end{bmatrix} = \begin{bmatrix} \lambda + 2\mu & \lambda & \lambda & 0 & 0 & 0 \\ \lambda & \lambda + 2\mu & \lambda & 0 & 0 & 0 \\ \lambda & \lambda & \lambda + 2\mu & 0 & 0 & 0 \\ 0 & 0 & 0 & \mu & 0 & 0 \\ 0 & 0 & 0 & 0 & \mu & 0 \\ 0 & 0 & 0 & 0 & 0 & \mu \end{bmatrix} \begin{bmatrix} \varepsilon_x \\ \varepsilon_y \\ \varepsilon_z \\ 2\gamma_{xz} \\ 2\gamma_{yx} \\ 2\gamma_{zy} \end{bmatrix} \tag{6}$$

where σ are stresses (MPa), ε are strains (-), τ and γ denote shear stress and shear strain, respectively (MPa). Indexes x, y, z denote the respective Cartesian directions.

In Eq. (1) the last term $\alpha_b \partial \varepsilon_{vol} / \partial t$ reflects the volume change of the porous medium, which is equivalent to adding or removing fluid. It can therefore be seen as a fluid source/sink term (Neuzil, 2012).

The volume or loading forces

$$\mathbf{f} = \alpha_b \rho_f g \nabla h \tag{7}$$

are evaluated as a vector in the centre of gravity. They represent the pore-pressure (Ingebritsen et al., 2006):

$$\sigma_{eff} = \sigma_{total} - \sigma_{pore} \tag{8}$$

In a THM problem the expansion of the rock matrix due to temperature changes has to be taken into account. Concomitant changes of the fluid properties are not discussed here because they are handled by FEFLOW directly (for details see Diersch and Kolditz, 2002). The volume of a solid increases or decreases with temperature changes, and homogenous bodies expand evenly in all directions when temperature increases. If deformation is not possible, the internal stresses increase or decrease with temperature changes (Kolditz et al., 2012). This unidirectional stress $\mathbf{f}'$ is added to the volume force following Ahola et al. (1996):

$$\mathbf{f}' = D \beta \Delta T \tag{9}$$

where β is the volumetric thermal expansion coefficient (K^{-1}), and D is the bulk modulus (Ingebritsen et al., 2006):

$$D = \lambda + \frac{2\mu}{3} = \frac{E}{3(1 - 2\upsilon)} \tag{10}$$

The hydraulic and mechanical equations are coupled because pore pressure appears in the linear elasticity equation, and because volumetric strain appears in the fluid-flow equation.

By consideration of the mechanical deformation, a non-linear system is resulting. This requires additional treatment in order to obtain convergence. The strain modifies the fluid-pressure, while the fluid-pressure is a force which is biasing the strain. Compared to the other TH coupled processes, mechanical compaction can be considered to be an instantaneous process (Kolditz et al., 2012). As stress and strain have a negligible impact on the temperature (Kolditz et al., 2012), a backward coupling with the temperature is not performed. Due to the strain, a change of the porosity and permeability is likely. This can be taken into account by reducing the porosity linearly with the change of volume and simultaneously changing the permeability in accordance with the porosity.

Finally the solute transport equation may be written as:

$$\frac{\partial \phi_e c}{\partial T} = \nabla \cdot (\phi_e D \nabla c - \mathbf{q} c) + Q \tag{11}$$

Where c is concentration (kg m^3), ϕ_e is effective porosity, D is the dispersion coefficient (m^2 s^{-1}), and Q are sources and sinks of dissolved substances (kg m^{-3} s^{-1}); all other symbols are according to the definitions given so far.

6. THMC MODELING OF A GEOTHERMAL DOUBLET SYSTEM

Figure 7 depicts the geometry of an idealized fracture-reservoir matrix system considered in the model by Ghassami and Kumar (2007) and Ghassemi et al. (2008). For the study presented here a similar approach has been selected.

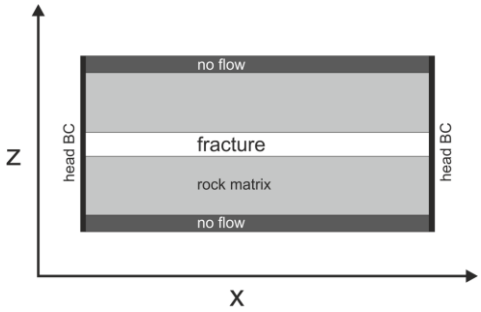

Figure 7: Idealized fracture-reservoir matrix system (modified from Ghassemi and Kumar, 2007). The left head boundary condition (BC) is simulating the injection by a borehole well, while the right head BC is an open boundary.

Based on the set-up shown in Figure 7 different effects which may influence the injectivity of a borehole are studied. Primarily the effect of thermo-elastic changes is considered here. Furthermore calcite solution is studied.

In this initial study the different effects are studied in an uncoupled manner with respect to their individual significance. Besides of the disadvantage of such an approach because nature simply is not uncoupled, the advantage is that it is easier to identify the relevance and potential contribution of the single processes.

6.1 Heat transport along a fracture and resulting thermo-elastic displacement

The model is a box with sides of 2 km times 2 km and a thickness of 200 m. The general model parameters are stated in Table 3. Horizontally in the middle of the model a fracture zone is included using a 2D discrete feature element (DFE). The DFE has a thickness of 5 mm and a hydraulic aperture of also 5 mm. The applied flow law is Hagen-Poiseuille (Diersch, 2014). The model has globally an initial temperature of 90 °C and a groundwater head of 0 m. After one day of simulation the head is increased for 10 m along a vertical central row; representing the injection into a borehole. For evaluating the respective injectivity the amount of water injected is compared (Table 4). The injected water has a temperature of only 40 °C.

Table 3: Physical properties used for the box model

Thermal conductivity of solid	2.2 W m^{-1} K^{-1}
Thermal conductivity of fluid	0.65 W m^{-1} K^{-1}
Volumetric heat capacity of solid	2.52 MJ m^{3} K^{-1}
Volumetric heat capacity of fluid	4.2 MJ m^{3} K^{-1}
Porosity	0.01
Hydraulic conductivity of matrix	$1 \cdot 10^{-8}$ m s^{-1}
Thermal expansion coefficient	$2 \cdot 10^{-6}$ K^{-1}
Young's module	46.53 GPa
Poisson ratio	0.1

For studying the effect of thermo-elastic deformation due to the injection of relatively cold water into the fracture a vertical cross-section of temperatures is extracted with a dimension of 100 m times 1 m, starting in the center (Figure 8). Due to symmetry of the problem only the lower part under the fracture is considered. The elastic deformation is computed with a modified MATLAB code from Alberty et al. (2002); thermo-elasticity is introduced according to Pepper and Heinrich (2005). The result is shown in Figure 10.

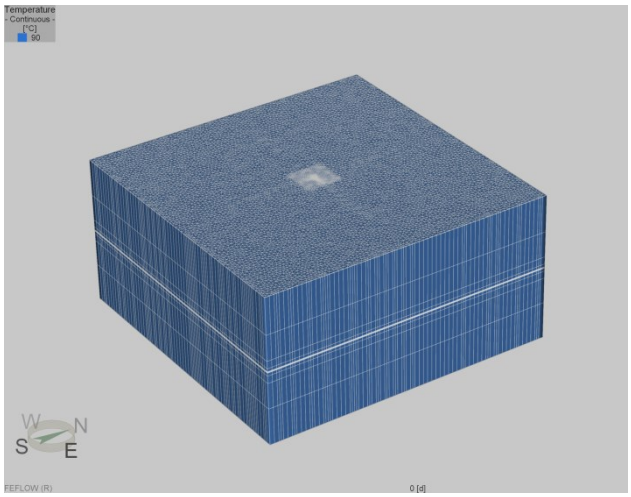

Figure 8 FEFLOW box model used for calculating heat-transport along a fracture.

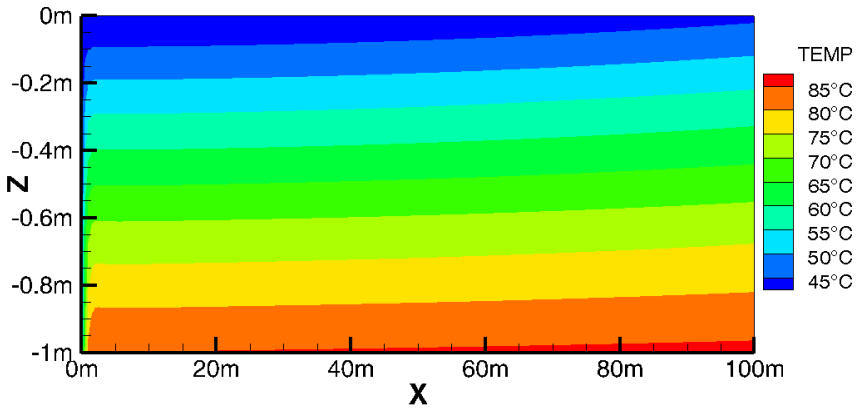

Figure 9 Temperature along the fracture (at the top) after 4 days of injection (the well is at the left axis).

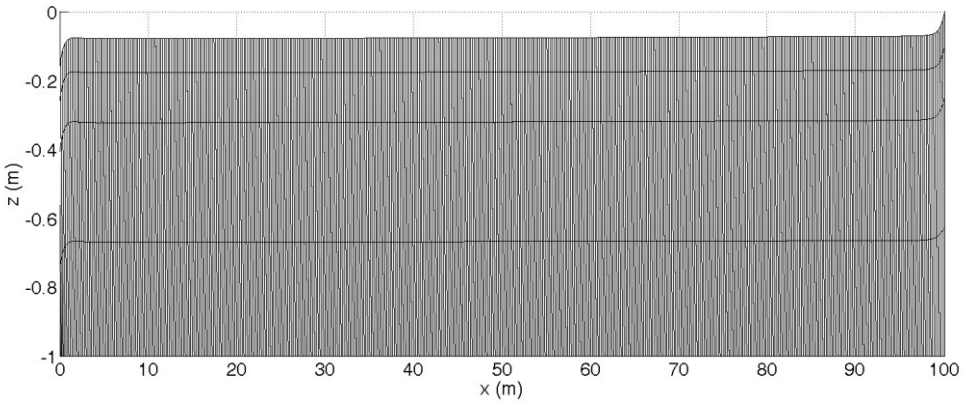

Figure 10: Deformation (10,000 times exaggerated) resulting from the temperature distribution shown in Figure 9.

Table 4: Flow rates after 0.5 days of injection.

Model type	Flow rate (l s^{-1})
Original model without thermo-elasticity	510
Model with thermo-elastic increased fracture aperture	512

A preliminary result of this study is that the impact of thermo-elasticity on the injectivity is small. However, of course the impact may be stronger for instance for smaller initial apertures or if a fracture network is considered.

6.2 Change of fracture conductivity due to calcite solution

The solution of calcite can be calculated using PHREEQC (Parkhurst and Appelo, 1999). Based on the solution presented by Merkel and Planer-Friedrich (2008) a matrix of solution indices (SI) as functions of temperature difference, distance along a 1D fracture can be derived (1).

A preliminary result is that the elapsed time has for the given flow velocity only a small impact while temperature difference and position along the fracture have a strong impact on the SI.

Using such a matrix a calcite solution can be introduced into a THMC numerical model without the need to compute a complete and costly chemical solution.

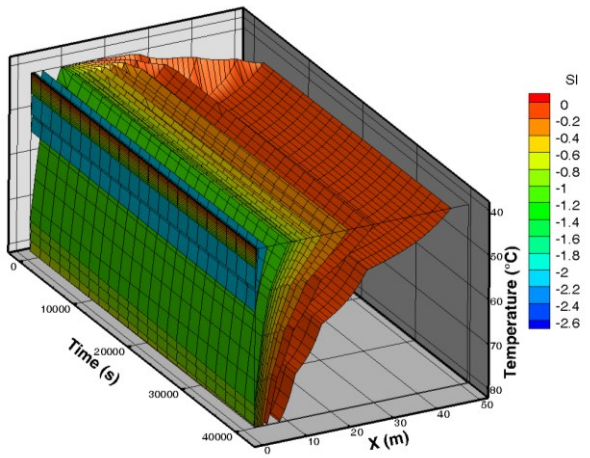

Figure 11: Solution indices calculated with PHREEQC for a 1D fracture of 50 m length in a limestone for different times (12 hours maximum) and different temperatures of the injected fluid. The rock matrix has always 90 °C. Depicted are different iso-surfaces according to the legend.

7. DISCUSSION AND OUTLOOK

Different physical and chemical effects can influence the wellbore injectivity in limestones. The study presented here summarizes the impact of the effect of thermo-elasticity. It shows a direction of how calcite solution could be considered in numerical modeling. Unconsidered here are the effects of hydro-mechanics, i.e. the opening of a fracture due to an increased fluid pressure; furthermore unconsidered is the effect of temperature on the fluids viscosity. All of these effects are strongly coupled in reality and the system of solutions is therefore non-linear.

Future work will include a fully coupled modeling of all processes discussed here, comparable to Rühaak and Sass (2013). By using the hydro-thermo-chemical simulator FEFLOW (Diersch, 2014) together with an extension for thermo- and hydro-mechanical coupling (Rühaak et al., 2014) the effect of thermo-elasticity, hydro-mechanics and temperature dependent fluid viscosity can be studied and compared with observed data. Furthermore, a simultaneous consideration of calcite solution will be enabled according to the approach presented here.

The coupled results will be presented at the World Geothermal Conference 2015 and compared with the uncoupled results shown here.

ACKNOWLEDGEMENTS

Liang Pei is funded by China Scholarship Council; this work is also financially supported by the DFG in the framework of the Excellence Initiative, Darmstadt Graduate School of Excellence Energy Science and Engineering (GSC 1070).

REFERENCES

Ahola, M.P., Thoraval, A., Chowdhury, A.H., 1996. Distinct Models for the Coupled T-H-M Processes: Theorie and Implementation. In: Coupled Thermo-Hydro-Mechanical Processes of Fractured Media. Mathematical and Experimental Studies. Recent Developments of DECOVALEX Project for Radioactive Waste Repositories. Stephansson, O., Jing, L., Tsang, C.-F. (Eds.). *Developments in Geotechnical Engineering*, 79, 181-212. doi:10.1016/S0165-1250(96)80026-5

Alam, M.M., Borre, M.K., Fabricius, I.L., Hedegaard, K., Røgen, B., Hossain, Z., and Krogsbøll, A.S., 2010. Biot's coefficient as an indicator of strength and porosity reduction: Calcareous sediments from Kerguelen Plateau. Journal of Petroleum Science and Engineering, 70(3-4), 282-297. doi:10.1016/j.petrol.2009.11.021

Alberty, J., Carstensen, C., Funken, S.A., and Klose, R.. Matlab Implementation of the Finite Element Method in Elasticity. *Computing*, **69**(3), (2002), 239-263. doi:10.1007/s00607-002-1459-8

Bear, J.: Dynamics of Fluids in Porous Media. Dover, New York, NY, (1972).

Biot, M.A.: General Theory of Three-Dimensional Consolidation. *Journal of Applied Physics*, **12**, (1941), 155-164.

Bundschuh, J., and Suárez Arriaga, M.C.: Introduction to the Numerical Modeling of Groundwater and Geothermal Systems: Fundamentals of Mass, Energy and Solute Transport in Poroelastic Rocks (Multiphysics Modeling), Taylor & Francis, Leiden, The Netherlands (2010).

Darrell W. Pepper and Juan C. Heinrich: The Finite Element Method: Basic Concepts and Applications, Second Edition, Taylor & Francis (2005).

Diersch, H.-J., G.: FEFLOW - Finite Element Modeling of Flow, Mass and Heat Transport in Porous and Fractured Media. 996 pp. Springer (2014).

Diersch, H.-J.G., and Kolditz O.: Variable-density flow and transport in porous media: approaches and challenges. Advances in Water Resources 25, 899-944 (2002).

Diersch, H.-J.G., and Perrochet, P.: On the primary variable switching technique for simulating unsaturated saturated flows. *Advances in Water Resources*, **23**(3), (1999), 271-301. doi:10.1016/S0309-1708(98)00057-8

Geyer, O.F., and Gwinner, M.P.: Die Schwäbische Alb und ihr Vorland. Slg. Geol. Führer 67. 271 pp, (1979).

Ghassemi, A. and Suresh Kumar, G.: Changes in fracture aperture and fluid pressure due to thermal stress and silica dissolution/precipitation induced by heat extraction from subsurface rocks, *Geothermics*, **36**(2), (2007), 115 – 140. doi: 10.1016/j.geothermics.2006.10.001

Ghassemi, A., Nygren, A., and Cheng, A.: Effects of heat extraction on fracture aperture: A poro-thermoelastic analysis, *Geothermics*, **37**(5), (2008), 525 – 539. doi: 10.1016/j.geothermics.2008.06.001

Gräf, V., Jamek, M., Rohatsch, A., and Tschegg, E.: Effects of thermal-heating cycle treatment on thermal expansion behavior of different building stones, *International Journal of Rock Mechanics and Mining Sciences*, **64**, (2013), 228 – 235. doi: 1016/j.ijrmms.2013.08.007

Gwinner, M.P.: Origin of the Upper Jurassic of the Swabian Alb. *Contrib. Sedimentol.*, **5**, (1976), 1-75.

Hegde, C., Rühaak, W., and Sass, I; Evaluation of Modelling of Flow in Fractures, Int. Conf. on Advances in Civil Engineering, AETACE, (2013). doi: 02.AETACE.2013.4.24

Homuth, S., Götz, A. E., and Sass, I.: Facies relation and depth dependency of thermo-and petrophysical rock parameters of the Upper Jurassic geothermal carbonate reservoirs of the Molasse Basin.- *Z. Dt. Ges. Geowiss*., (2014) (in press).

Ingebritsen, S.E., Sanford, W.E., and Neuzil, C.E.: Groundwater in Geologic Processes. 2nd Edition. Cambridge University Press, Cambridge, (2006).

Kinzelbach, W.: Numerische Methoden zur Modellierung des Transports von Schadstoffen im Grundwasser. 2nd Ed., Oldenbourg, (1992).

Kirkham, A.: A Quaternary proximal foreland ramp and its continental fringe, Arabian Gulf, UAE. *Geol. Soc. Spec. Publ.*, **149**, (1998), 15-41.

Kolditz, O., Görke, U.-J., Shao, H., and Wang, W.: Thermo-Hydro-Mechanical-Chemical Processes in Porous Media: Benchmarks and Examples. Springer, Heidelberg, (2012).

Lee, S. H., and Ghassemi, A.: Three-dimensional Thermo-Poro-Mechanical Modeling of Reservoir Stimulation and Induced Microseismicity in Geothermal Reservoir. *Proceedings*, Thirty-Sixth Workshop on Geothermal Reservoir Engineering, Stanford University, Stanford, California, (2011).

Leinfelder, R.R., Krautter, M., Laternser, R., Nose, M., Schmid, D.U., Schweigert, G., Werner, W., Keupp, H., Brugger, H., Herrmann, R., Rehfeld-Kiefer, U., Schroeder, J.H., Reinhold, C., Koch, R., Zeiss, A., Schweizer, V., Christmann, H., Menges, G., and Luterbacher, H.: The origin of jurassic reefs: current research developments and results. *Facies*, **31**, (1994), 1-56.

Leinfelder, R.R., Werner, W., Nose, M., Schmid, D.U., Krautter, M., Laternser, R., Takacs, M., and Hartmann, D.: Paleoecology, Growth Parameters and Dynamics of Coral, Sponge and Microbolite Reefs from the Late Jurassic. *Göttinger Arb. Geol. Palaentol*. Sb, **2**, (1996), 227– 248.

Merkel, B. J., and Planer-Friedrich, B.: Grundwasserchemie, Springer-Verlag Berlin Heidelberg, (2008).

Meyer, R.K.F., Schmidt-Kaler, H.: Paläogeographie und Schwammriffentwicklung des süddeutschen Malm - ein Überblick. *Facies*, **23**, (1990), 175-184.

Meyer, R.K.F., Schmidt-Kaler, H.: Paläogeographischer Atlas des süddeutschen Oberjura (Malm). *Geol. Jb*. **A/115**, (1989), 3-77.

Nasseri, M.H.B, Goodfellow, S.D., Wanne, T. and Young, R.P.: Thermo-hydro-mechanical properties of Cobourg limestone, *International Journal of Rock Mechanics and Mining Sciences*, **61**, (2013), 212-222. doi: 10.1016/j.ijrmms.2013.03.004.

Neuzil, C.E.,: Hydromechanical effects of continental glaciation on groundwater systems. *Geofluids*, **12**(1), (2012), 22-37. doi:10.1111/j.1468-8123.2011.00347.x

Parkhurst, D.L. and Appelo, C.A.J.: User's guide to PHREEQC (version 2). US Geol. Surv. Water Resour. Inv. Rep. 99-4259, 312p, (1999).

Pawellek, T. and Aigner, T.: Apparently homogenous „reef"-limestones built by high-frequency cycles Upper Jurassic, SW-Germany. *Sediment. Geol.*, **160**, (2003), 259-284.

Pawellek, T.: Fazies-, Sequenz-, und Gamma-Ray-Analyse im höheren Malm der Schwäbischen Alb (SW-Deutschland) mit Bemerkungen zur Rohstoffgeologie (hochreine Kalke), *Tübinger Geol. Arb.*, **Reihe A 61**, (2001), 1-246.

Pei, L., Mielke, P., Rühaak, W., Stegner, J., Homuth, S., Bär, K., and Sass, I.: Thermo-Triax: An Apparatus for Testing Petrophysical Properties of Rocks under Simulated Geothermal Reservoir Conditions (2014, in review).

Pieńkowski, G., Schudack, M. E., Bosák, P., Enay, R., Feldman-Olszewska, A., Golonka, J., Gutowski, J., Herngreen, G. F. W., Jordan, P., Krobicki, M., Lathuilière, B., Leinfelder, R.R., Michalík, J., Mönnig, E., Noe-Nygaard, N., Pálfy, J., Pint, A., Rasser, M.W., Reisdorf, A.G., Schmid, D.U., Schweigert, G., Surlyk, F., Wetzel, A. and Wong, T.E.: Jurassic. - In: McCann, T. (ed.): The Geology of Central Europe. - Volume 2: Mesozoic and Cenozoic: 823-922, London (The Geological Society), (2008).

Rühaak, W., and Sass, I.: Applied Thermo-Hydro-Mechanical Coupled Modeling of Geothermal Prospection in the Northern Upper Rhine Graben. *Proceeding,* Thirty-Eighth Workshop on Geothermal Reservoir Engineering, Stanford University, Stanford, California, February 11 - 13, SGP-TR-198, (2013).

Rühaak, W., Bense, V. F. and Sass, I.: 3D hydro-mechanically coupled groundwater flow modelling of Pleistocene glaciation effects. *Computers & Geosciences*, **67**, (2014), 89 – 99

Rühaak, W., Rath, V., Wolf, A., and Clauser, C.: 3D finite volume groundwater and heat transport modeling with non-orthogonal grids using a coordinate transformation method. *Advances in Water Resources*, **31**(3), (2008), 513-524.

Selg, M. and Wagenplast, P.: Beckenarchitektur im süddeutschen Weißen Jura und die Bildung der Schwammriffe. *Jh. Geol. Landesamt Baden-Württemberg*, **32**, (1990), 171-206.

Snow, D.: A parallel plate model of fractured permeable media, Ph.D. thesis, University of California, Berkeley, USA, (1965).

Villinger, E.: Hydrogeologische Ergebnisse. In: Bertleff, B. et al.: Ergebnisse der Hydrogeothermiebohrungen in Baden-Württemberg. *Jh. d. Geol. Landesamtes Baden-Württemberg*, **30,** (1988), 27-116.

Wang, H.F.: Theory of Linear Poroelasticity – with Applications to Geomechanics and Hydrogeology. Princenton University Press, Princeton, NJ, (2000).

Wang, W., Kosakowski, G., and Kolditz, O.: A parallel finite element scheme for thermo-hydro-mechanical (THM) coupled problems in porous media, *Computers & Geosciences*, **35**(8), (2009), 1631-1641. doi:10.1007/s00466-009-0445-9

Watanabe, N., Wang, W., McDermott, C., Taniguchi, T., and Kolditz, O.: Uncertainty analysis of thermo-hydro-mechanical coupled processes in heterogeneous porous media. *Computational Mechanics*, **45**(4), (2010), 263-280. doi:10.1007/s00466-009-0445-9

Watanabe, N., Wang, W., Taron, J., Görke, U. J. and Kolditz, O.: Lower-dimensional interface elements with local enrichment: application to coupled hydro-mechanical problems in discretely fractured porous media, *International Journal for Numerical Methods in Engineering*, **90**(8), (2012), 1010-1034. doi:10.1002/nme.3353

Wijesinghe, A. M. An exact similarity solution for coupled deformation and fluid flow in discrete fractures. Technical Report UCID–20675, Lawrence Livermore National Laboratory, Livermore, CA, February (1986).

Wright, V.P., and Burchette, T.P.: Carbonate ramps. *Geol. Soc. Spec. Publ*., **149**, (1998), 1-397.